Phase stability of terawatt-class ultrabroadband parametric amplification

Renault, A.A.L.; Kandula, D.Z.; Witte, S.; Wolf, A.L.; Zinkstok, R.T.; Hogervorst, W.;
Eikema, K.S.E.

published in
Optics Letters
2007

DOI (link to publisher)
10.1364/OL.32.002363

document version
Publisher's PDF, also known as Version of record

Phase stability of terawatt-class ultrabroadband parametric amplification

A. Renault, D. Z. Kandula, S. Witte, A. L. Wolf, R. Th. Zinkstok, W. Hogervorst, and K. S. E. Eikema*

Atomic, Molecular, and Laser Physics Group, Laser Centre Vrije Universiteit, De Boelelaan 1081, 1081 HV Amsterdam, The Netherlands
**Corresponding author: kjeld@nat.vu.nl*

Received May 9, 2007; revised June 15, 2007; accepted June 18, 2007; posted June 20, 2007 (Doc. ID 82839); published August 2, 2007

The phase stability of broadband (280 nm bandwidth) terawatt-class parametric amplification was measured, for the first time to our knowledge, with a combination of spatial and spectral interferometry. Measurements at four different wavelengths from 750 to 900 nm were performed in combination with numerical modeling. The phase stability is better than 1/23 rms of an optical cycle for all the measured wavelengths, depending on the phase-matching conditions in the amplifier.
OCIS codes: 190.4970, 320.7090, 320.7160, 350.5030.

The generation and amplification of phase-controlled few-cycle laser pulses is a necessity for applications such as quantum interference metrology [1], attosecond science [2], and quantum control of, e.g., molecular dynamics [3]. Intense, phase-stable few-cycle laser pulses have been produced by using Ti:sapphire amplifiers and subsequent spectral broadening in filaments. However, filamentation in gas-filled hollow fibers [4], or directly in a gas cell [5], is difficult to scale beyond ≈ 0.2 TW. In parametric amplification phase-stable pulses, albeit at moderate energies of a few hundred microjoules [6–9], have also been demonstrated. The generation of multimillijoule-level phase-controlled few-cycle pulses with terawatt (TW) intensity has not been demonstrated to date.

In this Letter we report what is, to the best of our knowledge, the first measurement of the phase stability of TW-class ultrafast amplification. The amplifier is based on noncollinear optical parametric chirped pulse amplification (NOPCPA) and was described elsewhere in detail [10]. It consists of a double-pass preamplifier and a single-pass power amplifier using BBO crystals. The seed laser is a home-built 6.2 fs frequency comb oscillator, producing phase-locked 5.5 nJ pulses at a 75 MHz repetition rate. The carrier-envelope phase (CEP) stability of the oscillator is 1/46 rms of an optical cycle. The 532 nm pump laser provides 170 mJ pulses with a duration of 60 ps and is synchronized to the oscillator laser. The system operates at a repetition rate of 30 Hz and is capable of generating 7.6 fs pulses at 2 TW (15.5 mJ after compression) when the normal full seed energy of 1 nJ per pulse is available.

The phase stability of the NOPCPA output is measured with linear interferometry. The advantage of this method over the frequently used f:$2f$ technique [11] is that pulse intensity fluctuations (typically a few percent) do not influence the measurement; also the wavelength dependence can be measured. The system is based on a double interferometer, to be able to correct for optical path fluctuations due to external noise and drift (see Fig. 1). The interferometer path length variations, of the order of a wavelength, are too small to influence the CEP. Changes induced by thermal effects due to the 20 mm of optical material in the NOPCPA path are small and are in addition compensated by a similar amount of material in the reference arm. The interferometer compares interference [12] between parametrically amplified and nonamplified frequency comb pulses with a spatial interference pattern generated by a reference He–Ne laser beam traveling the same path as the IR light. About 50% of the IR seed light is split off (0.5 nJ) behind the stretcher as a phase reference; the He–Ne laser is coupled in both arms via this beam splitter. Several telescopes are used to match the beam parameters for the He–Ne laser and the IR beam at the end of the interferometer. The remaining 0.5 nJ of the IR seed light is amplified in the NOPCPA up to 23 mJ at a 30 Hz repetition rate with a 280 nm wide spectrum. Because of the reduced seeding to the amplifier, this is slightly less than reported before [10], but still sufficient to generate pulses exceeding 1 TW. The pulses are measured before the compressor to avoid nonlinear effects in the interferometer in order to measure only the influence of parametric amplification. Negligible additional phase noise is expected

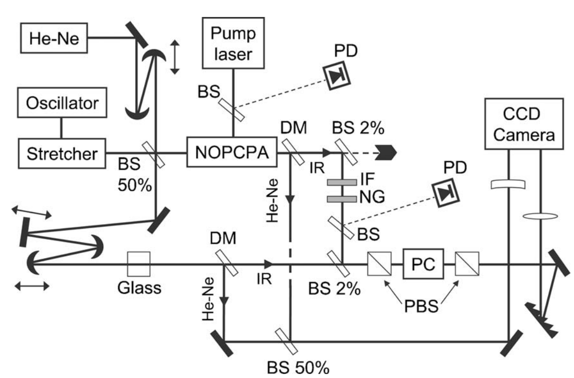

Fig. 1. Setup used to measure the phase stability of the TW NOPCPA system. The path through the NOPCPA is 5 m, while the recombination section is in reality only a few tens of centimeters. BS, beam splitter; DM, dichroic mirror; PD, photodiode; IF, interference filter; NG, neutral gray filter; PBS, polarizing beam splitter; PC, Pockels cell; IR, infrared beam; G, grating 1200 lines/mm.

from the compressor, given its stable construction and small compression ratio of 1:2000 [13].

Both the IR and He–Ne laser beams are recombined individually with their respective reference beams behind the amplifier. The IR beam is attenuated by using 2% beam splitters and a 10^{-5} filter to match the intensity with that of the reference pulses. Also, an interference filter is inserted here (bandwidth 10 nm, with a wavelength centered at either 750, 795, 850, or 900 nm), so that the wavelength dependence can be investigated. A home-built spectrometer is used to measure spectral fringes from the IR pulses on a CCD. The delay between amplified and reference pulses is set such that as many as 10 fringes are visible over the 10 nm bandwidth. A spatial interference pattern is recorded on the same CCD as a length reference by recombining the He–Ne laser beams at a small angle on a 50% beam splitter.

Measurements of the phase are performed by recording every third pulse of the amplifier for several minutes. The phase is extracted from the two interference patterns by using a Fourier method described in [14], taking the difference in wavelength between the He–Ne and the amplified beam into account. In Fig. 2 the result is shown for a typical measurement at 850 nm. The pump laser intensity stability is 1% in this case, while the amplifier output stability ranges from 6% at 750 nm to 1.3% at 900 nm. The IR and He–Ne phase individually fluctuate because of external influences, but the difference is rather stable. With the NOPCPA switched off, a minimum phase noise detection limit of 0.09 rad (rms) is found at 795 nm. For the measurement of Fig. 2, correcting for this detection limit, a rms phase noise of 0.27 rad at 750 nm, 0.23 rad at both 795 and 850 nm, and 0.10 rad at 900 nm (1/63 of an optical cycle) results.

Theoretically the phase of the amplified beam is influenced mostly by the parametric process itself and slightly by (cross-)phase modulation due to nonlinear refractive index effects. For the latter, phase fluctuations of the order of 0.01 rad are expected, based on a calculated nonlinear phase shift of 0.36 rad for the amplifier and a pump intensity variation of a few percent. The influence on the phase of the signal beam due to parametric amplification is given by [15]

$$\varphi_s(L) = \varphi_s(0) - \frac{\Delta k}{2}\int_0^L \frac{f}{f+\gamma_s^2}\mathrm{d}z. \tag{1}$$

Here $f=1-I_p(z)/I_p(0)$ is the fractional pump intensity depletion, and $\gamma_s^2=\omega_p I_s(0)/\omega_s I_p(0)$. In this expression L is the interaction length, Δk is the phase mismatch, I_s is the seed intensity, and ω_s and ω_p are the seed and pump frequencies. Equation (1) states that there is a coupling between the pump intensity and the phase of the seed pulse. To estimate the influence of this effect, numerical simulations have been performed for a three-pass NOPCPA system using a split-step Fourier algorithm [16]. In Fig. 3 the results are shown for the calculated phase-matching conditions and shifts, together with the calculated and experimental spectrum for the measurement depicted in Fig. 2. From Fig. 3 it can be seen that the pump-induced phase shifts are proportional to $-\Delta k$, as predicted by Eq. (1).

A direct quantitative comparison with the experiment is hampered by the extreme sensitivity of Δk to the angles in the three different amplifier passes. This means that the experimental Δk is difficult to determine. It is, however, clear that the calculated phase shifts as a function of pump-power variations are several times lower than the typical values seen in the experiment, especially at 750 nm. We attribute this to a combination of slightly differently aligned

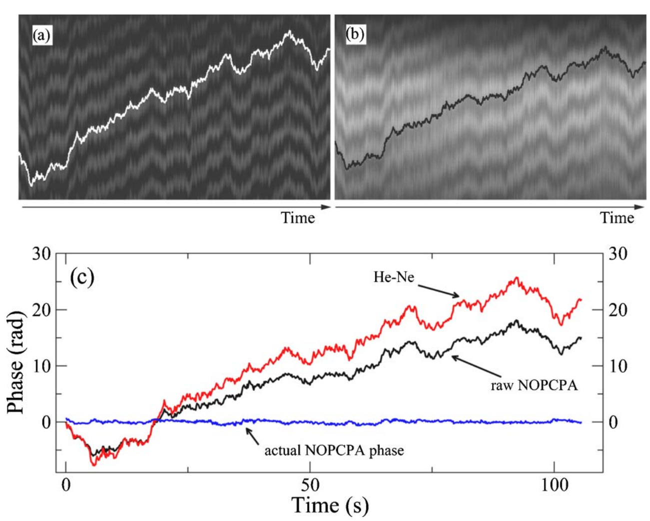

Fig. 2. (Color online) Evolution in time of the interference pattern for (a) He–Ne and (b) NOPCPA (λ=850 nm) together with the derived phase traces, which are also depicted in (c) (He–Ne, red; raw NOPCPA, black), as well as the corrected phase noise of the NOPCPA (see text).

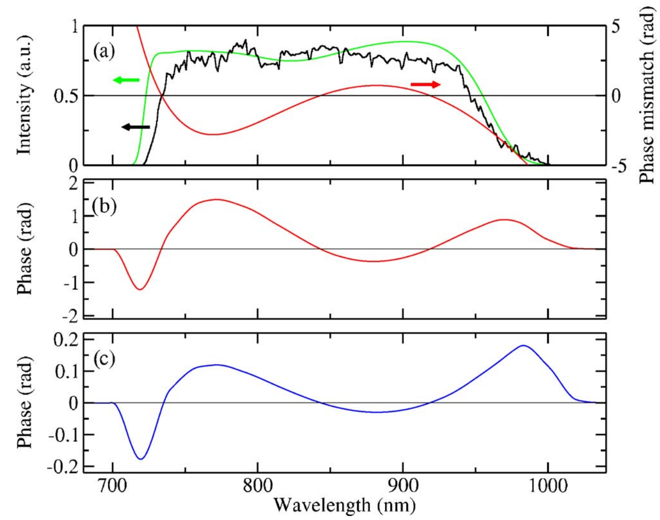

Fig. 3. (Color online) (a) Measured spectrum of the amplified NOPCPA output (black trace), along with a simulated spectrum for phase-matching angle $\theta=23.887°$ and noncollinear angle $\alpha=2.40°$ (green or light gray curve) and the phase mismatch curve ΔkL for a 5 mm long BBO crystal with the phase-matching angles as used in the simulation (red or thin black curve). (b) Total pump-induced phase shift introduced by a complete pass through the amplifier according to Eq. (1). (c) Wavelength-dependent phase shift resulting from a 5% increase in pump intensity.

passes (leading to larger Δk), possible (pump) beam pointing fluctuations, and the influence of pulse-to-pulse intensity variations on the phase readout.

To detect the correlation between the (pump) intensity and the phase we use Spearman's rank correlation coefficient (RC), as it is particularly suited for noisy datasets [17]. An RC of (−)1 signifies full (anti) correlation, while 0 means no correlation. With sufficient gain the RC should in principle increase for a larger Δk, and change sign together with Δk. For the spectrum shown in Fig. 3 no significant correlation could be detected between pump intensity and output phase. However, the situation is different when the NOPCPA is less well aligned, leading to a bigger Δk and a strongly modulated spectrum. Significant (anti)correlations can then sometimes be observed, such as the case where the phase-pump intensity RC changes sign from +0.4 at 750 nm to −0.3 at 795 nm. In this situation oversaturation (backconversion) was observed at 795 nm. At other wavelengths the RC is normally too small to draw conclusions.

To further study the Δk effects at a fixed wavelength of 795 nm, we deliberately induced a strong phase mismatch by rotating the last crystal from $\theta \approx 23.8°$ to $\theta + 0.06°$. The pump intensity was modulated by about 10% to make the measurement more sensitive to correlations. The result is shown in Fig. 4; the RC changed sign from +0.4 to −0.2, in qualitative agreement with simulations. A strikingly big phase jump of 1.7 rad is seen that is not present when the NOPCPA system is switched off. Such a big phase shift is theoretically possible if the integral in Eq. (1) would stay large for a big Δk. This can be explained by assuming an average pump power of $7\ \mathrm{GW/cm^2}$ (20% higher than initially estimated).

In conclusion, we demonstrated phase-stable TW-class parametric amplification for the first time. On average the phase stability is better than 1/25 of an optical cycle across the amplified spectrum for the measured pump laser fluctuations of 1% rms. The measured phase noise is several times larger than numerically simulated, but qualitative agreement is found for the expected Δk dependence. The average phase stability of 1/25 of an optical cycle gives an upper bound for the influence on the carrier-envelope phase when the pulses would be fully compressed, demonstrating that TW peak power few-cycle laser pulses can be produced with NOPCPA.

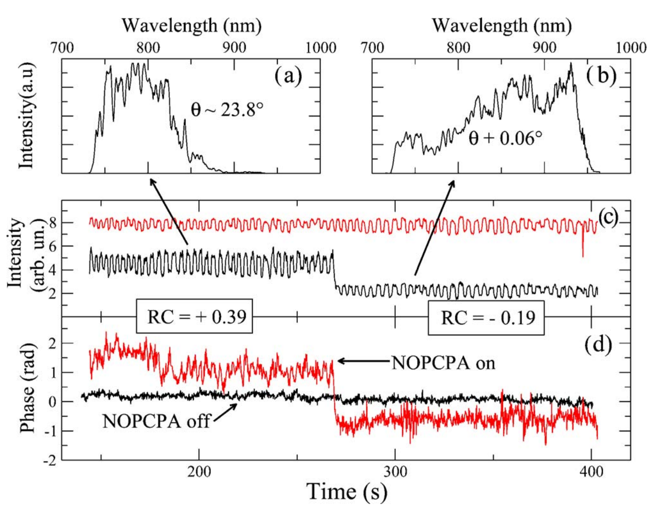

Fig. 4. (Color online) Influence of the phase-matching angle on the phase of the NOPCPA. (a), (b) NOPCPA spectra for two different phase-matching angles, separated by 0.06°. (c) NOPCPA intensity at 795 nm (black) and pump intensity (red or gray). (d) Phase evolution with (red or gray) and without (black) the NOPCPA switched on (For RC between pump intensity and phase, see text).

We gratefully acknowledge financial support by the Netherlands Organization for Scientific Research (NWO), the EU Integrated Initiative FP6 program Laserlab-Europe, and the Industrial Partnership Programme (IPP) Metrology with Frequency Comb Lasers (MFCL) supported by the Foundation for Fundamental Research on Matter (FOM).

References

1. S. Witte, R. Th. Zinkstok, W. Ubachs, W. Hogervorst, and K. S. E. Eikema, Science **307**, 400 (2005).
2. A. Baltuška, Th. Udem, M. Uiberacker, M. Hentschel, E. Goulielmakis, Ch. Gohle, R. Holzwarth, V. S. Yakovlev, A. Scrinzi, T. W. Hänsch, and F. Krausz, Nature **421**, 611 (2003).
3. M. F. Kling, Ch. Siedschlag, A. J. Verhoef, J. I. Khan, M. Schultze, Th. Uphues, Y. Ni, M. Uiberacker, M. Drescher, F. Krausz, and M. J. J. Vrakking, Science **312**, 246 (2006).
4. A. J. Verhoef, J. Seres, K. Schmid, Y. Nomura, G. Tempea, L. Veisz, and F. Krausz, Appl. Phys. B **82**, 513 (2006).
5. C. P. Hauri, W. Kornelis, F. W. Helbing, A. Heinrich, A. Couairon, A. Mysyrowicz, J. Biegert, and U. Keller, Appl. Phys. (N.Y.) **79**, 673 (2004).
6. A. Baltuška, T. Fuji, and T. Kobayashi, Phys. Rev. Lett. **88**, 133901 (2002).
7. C. Vozzi, G. Cirmi, C. Manzoni, E. Benedetti, F. Calegari, G. Sansone, S. Stagira, O. Svelto, S. De Silvestri, M. Nisoli, and G. Cerullo, Opt. Express **14**, 10109 (2006).
8. C. P. Hauri, P. Schlup, G. Arisholm, J. Biegert, and U. Keller, Opt. Lett. **29**, 1369 (2004).
9. R. Th. Zinkstok, S. Witte, W. Hogervorst, and K. S. E. Eikema, Opt. Lett. **30**, 78 (2005).
10. S. Witte, R. Th. Zinkstok, A. L. Wolf, W. Hogervorst, W. Ubachs, and K. S. E. Eikema, Opt. Express **14**, 8168 (2006).
11. M. Kakehata, H. Takada, Y. Kobayashi, K. Torizuka, Y. Fujihira, T. Homma, and H. Takahashi, Opt. Lett. **26**, 1436 (2001).
12. L. Lepetit, G. Chériaux, and M. Joffre, J. Opt. Soc. Am. B **12**, 2467 (1995).
13. I. Thomann, E. Gagnon, R. J. Jones, A. S. Sandhu, A. Lytle, R. Anderson, J. Ye, M. Murnane, and H. Kapteyn, Opt. Express **12**, 3493 (2004).
14. M. Takeda, H. Ina, and S. Kobayashi, J. Opt. Soc. Am. **72**, 156 (1982).
15. I. N. Ross, P. Matousek, G. H. C. New, and K. Osvay, J. Opt. Soc. Am. B **19**, 2945 (2002).
16. S. Witte, R. Th. Zinkstok, W. Hogervorst, and K. S. E. Eikema, Appl. Phys. B **87**, 677 (2007).
17. W. H. Press, B. P. Flannery, S. A. Teukolsky, and W. T. Vetterling, *Numerical Recipes in C: the Art of Scientific Computing* (Cambridge U. Press, 1992).